Obrabotka metallov –
Metal Working and Material Science

Journal homepage: http://journals.nstu.ru/obrabotka_metallov

Predicting machined surface quality under conditions of increasing tool wear

Victor Lapshin [a, *], *Alexandra Gubanova* [b], *Ilya Dudinov* [c]

Don State Technical University, 1 Gagarin square, Rostov-on-Don, 344000, Russian Federation

[a] https://orcid.org/0000-0002-5114-0316, ✉ lapshin1917@yandex.ru; [b] https://orcid.org/0000-0002-9785-5384, ✉ anatoliya81@mail.ru;
[c] https://orcid.org/0009-0009-0784-1287, ✉ ilya.sandman@yandex.ru

ARTICLE INFO

ABSTRACT

Introduction. The most important factor determining the efficiency of metal cutting is the quality of the surface of the part obtained during cutting. The surface quality of a machined part is directly dependent on the vibration activity of the cutting tool, the amplitude of which is influenced by the complex evolutionary dynamics of the cutting process. In light of this, modern digital twin technology, which allows predicting the surface quality values of the parts using virtual models, is becoming an extremely relevant way to improve the efficiency in metalworking control systems. **The purpose of the work.** This study aims to improve the prediction accuracy of a digital twin system for the surface quality of the machined parts under conditions of increasing cutting tool wear. **The paper examines:** the dynamics of the turning process of metal parts, as well as a mathematical model describing the dynamics of tool vibrations during metal machining on lathes, considering the influence of the thermodynamic subsystem of the cutting system. **Research methods.** An experimental approach was employed, utilizing a author-designed measuring stand along with a modern inverted metallographic microscope *LaboMet-I* version 4, equipped with wide-angle lenses 5/20, having a 20 mm linear field of view, and a digital camera for microscopes *Ucam-1400* with a 1.4 μm×1.4 μm matrix, and a contour profile recorder *T4HD*. Furthermore, the study used mathematical modeling of the dynamic cutting system in the *Matlab* environment, for which the authors developed a specialized data processing program. **Results and discussion.** Curves depicting the tool wear rate, changes in the quality parameters of the machined surface as functions of cutting path, and as a function of cutting tool wear are constructed. Dynamic indicators suitable for parametric identification of virtual digital twin models are determined. The structure of these models is established, and parametric identification is performed. Numerical modeling is conducted in the *Matlab* environment, based on the results of which a curve depicting the change in average arithmetic surface roughness as a function of increasing tool wear is constructed. The convergence of the results of field and numerical experiments is evaluated, which shows a high reliability of the surface quality prediction achievable through the use of digital twin systems.

Introduction

As is well known, improving the quality of metal part processing on metal-cutting machines can be achieved by increasing positioning accuracy or by reducing vibrations of both the cutting tool and the workpiece, which is fixed in the machine's spindle [1]. A crucial factor determining the surface quality during cutting is the wear of the cutting tool. A particularly problematic situation arises when the tool reaches critical wear values, leading to a sharp increase in vibration activity and, consequently, a decrease in the obtained surface quality. Therefore, assessing the impact of cutting tool wear on the surface quality achieved during machining is a urgent scientific task.

* Corresponding author
Lapshin Viktor P., Ph.D. (Engineering), Associate Professor
Don State Technical University,
1 Gagarin square,
344000, Rostov-on-don, Russian Federation
Tel.: +7 900 122-75-14, **e-mail:** lapshin1917@yandex.ru

In contemporary view, vibration monitoring systems enable the prediction of surface quality during cutting based on digital vibration measurements [2-3]. However, such prediction relies on the development of complex mathematical models that capture the evolutionary dynamics of the cutting process [4]. The complexity of these models and the requirement for their parametric identification present a significant challenge. Addressing this challenge will substantially enhance the capabilities of modern metalworking systems. One promising solution involves leveraging a novel digital paradigm in metalworking control systems known as the "*digital twin*" [5-7]. Specifically, the application of intelligent models that describe the complex dynamics of technological processes during metal cutting holds significant potential in this emerging field of scientific knowledge [8-9].

For example, the work by *Y. Altintas* and his research groups, prominent experts in the field of digital twin-based metalworking control, proposes using digital twins to generate new *CNC* programs that allow part machining without preliminary setups and experiments [10]. This suggests that the selection of optimal processing modes, both in addressing current challenges and in reconfiguring the control system on a metal-cutting machine (i.e., achieving flexibility), can be achieved using virtual models within a digital twin. From a modern perspective, the technology of constructing digital twins, particularly the synthesis of virtual models, relies on two primary paradigms: one based on deterministic mathematical models [10] and the other on the widespread use of neural networks [8-9].

A critical direction in the development of digital twin technology is the diagnosis of various malfunctions. For instance, in [11], the focus is on generating labeled training datasets for various bearing malfunctions to supplement limited measured data. The authors propose a novel digital twin approach to address the scarcity of measured data in bearing malfunction diagnosis. Experimental results demonstrate an increase in the accuracy of malfunction diagnosis [12]. A similar perspective, albeit with slight variations, is presented in [13]. The authors highlight the limitations of traditional malfunction diagnosis methods that rely on experimental data, noting that in mission-critical industrial scenarios, such data is not always available. Digital twin technology, by creating a virtual representation of a physical object that reflects its operating conditions, enables the diagnosis of technical system or technological process malfunctions even when insufficient data on those malfunctions exists. The authors propose a malfunction diagnosis system based on digital twins that leverages labeled simulated data and unlabeled measured data [13]. The construction of a digital twin system that integrates sensor data from malfunctioning bearings into the subspaces of virtual models in real time is presented [14]. The authors refine the parameters of the virtual models by comparing the results of digital modeling in the time domain with the measured and captured signals [14].

At the same time, accurately modeling the complex influence of cutting tool wear on the dynamics of the cutting process remains an extremely challenging task, which cannot be solved without considering the thermodynamic aspects of the processes occurring during metal cutting [15-16]. Based on the analysis, digital twin technology has become widely adopted in the diagnosis of malfunctions, including bearing malfunctions. Therefore, an obvious development of digital twin technology is to leverage it for predicting the impact of cutting tool wear on the quality of the parts produced during machining.

Based on this, we formulate the ***purpose of the study*** as improving the accuracy of the digital twin system's prediction of surface quality during machining under conditions of progressive cutting tool wear through parametric identification of the digital twin's virtual models using data obtained from a vibration monitoring system of the cutting process.

Research methodology

Vibration monitoring system for assessing cutting tool wear and machined surface quality

The experimental component of this research utilizes a vibration diagnostic subsystem, positioned on the cutting tool itself, or rather on its holder, as depicted in Fig. 1. This system is based on an industrial *IEPE* (*ICP*) general-purpose accelerometer with an integrated *A603C01T* charge converter amplifier. The accelerometer has a frequency range of $+/-$ 3 dB: 0.4-15,000 Hz; a sensitivity of $+/-$ 10 %: 10.2 mV/(m/s^2). The system also includes a single-channel *ICP* (*IEPE*) converter with a frequency range of 0.1-50,000 Hz.

a

b
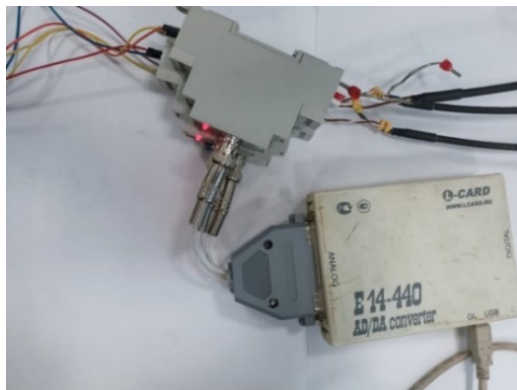
c

d

Fig. 1. Vibration monitoring system on the *1K625* lathe:
a, *b* – industrial accelerometers; *c*, *d* – amplifier converter and *ADC*

As can be seen from Fig. 1, the vibration monitoring system relies on piezoelectric vibration sensors of the cutting tool. However, new intelligent sensors are becoming increasingly prevalent, offering the capability to digitally display vibration accelerations, speeds, and tool displacements directly [17-20].

To illustrate the system's operation, consider a turning example where a steel shaft (steel 45) with a diameter of 50 mm was machined on a *1K625* lathe. The processing mode was: a cutting speed of 124 m/min, a depth of cut of 1 mm, and a feed rate of 0.11 mm/rev. We performed sequential double integration of the measured vibration acceleration signals using a program written in the *Matlab* environment.

The resulting vibration acceleration signals from the *x*, *y*, and *z* channels, along with the calculated vibration velocity and displacement values, are presented for a single measurement case in the aforementioned figures.

The adequacy of the program for step-by-step integration of the captured vibration acceleration signal can be conveniently examined by analyzing the main carrier frequencies in the signal's spectrum, as illustrated in Fig. 5.

As observed in Fig. 5, the main carrier frequencies remain unchanged. However, the high-frequency component of the vibration signal is significantly attenuated. This attenuation is attributed to the fact that the integration process involves summation and averaging operations, which aligns with the inertial properties of the object (tool).

The actual wear of the cutting tool can be influenced by random factors not accounted for in digital twin mathematical models. To assess the actual wear of the cutting tool, a separate experiment was conducted on the *1K625* lathe, machining the shaft (steel 45) using the previously specified cutting mode. To measure
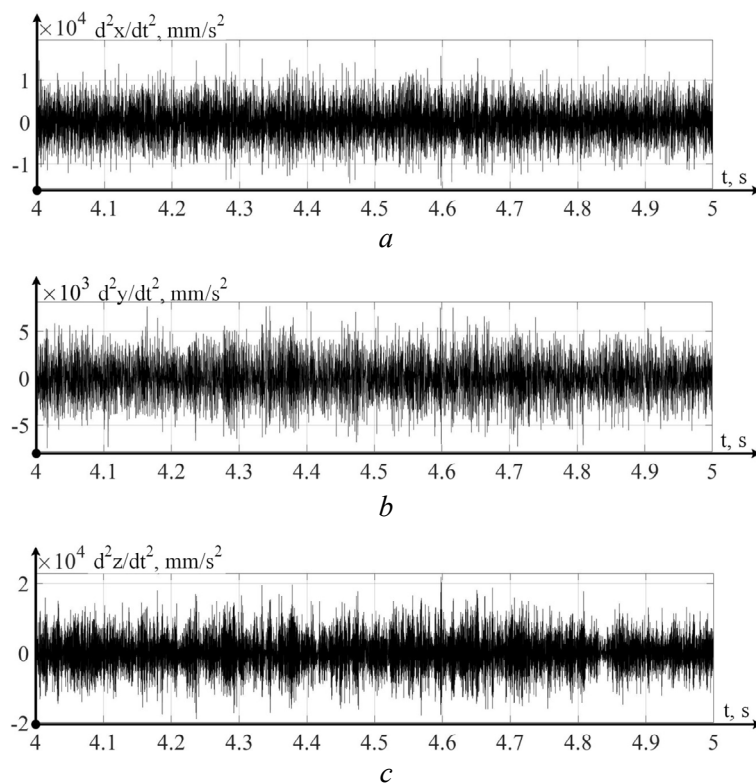
Fig. 2. Vibration acceleration signals for cutting at a speed of 150 m/min:

a – in the axial direction; b – in the radial direction;
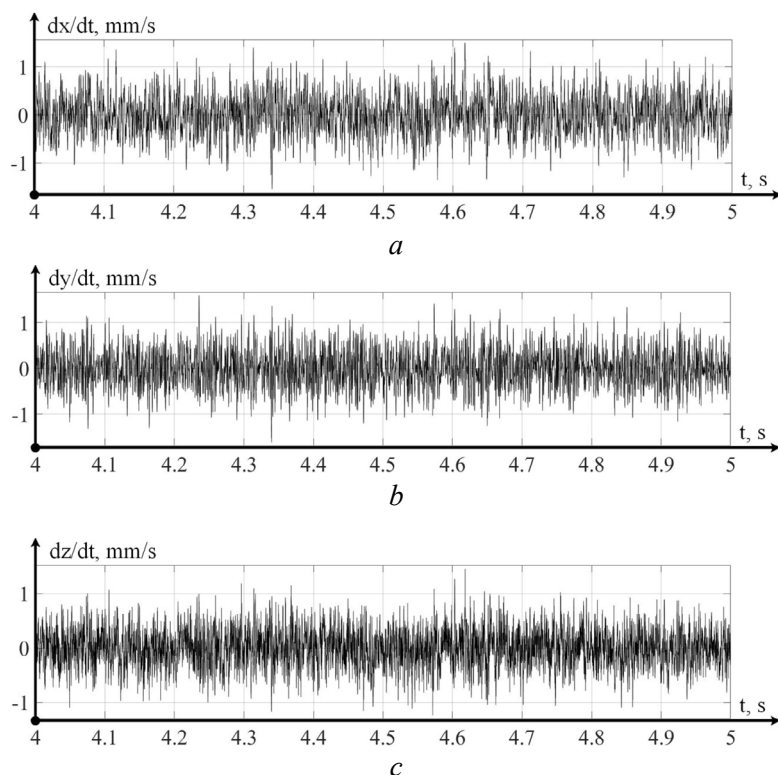c – in the tangential direction

Fig. 3. Vibration velocity signals for cutting at a speed of 150 m/min:

a – in the axial direction; b – in the radial direction; c – in the tangential direction

Fig. 4. Vibration displacement signals for cutting at a speed
of 150 m/min:

a – in the axial direction; *b* – in the radial direction;
c – in the tangential direction

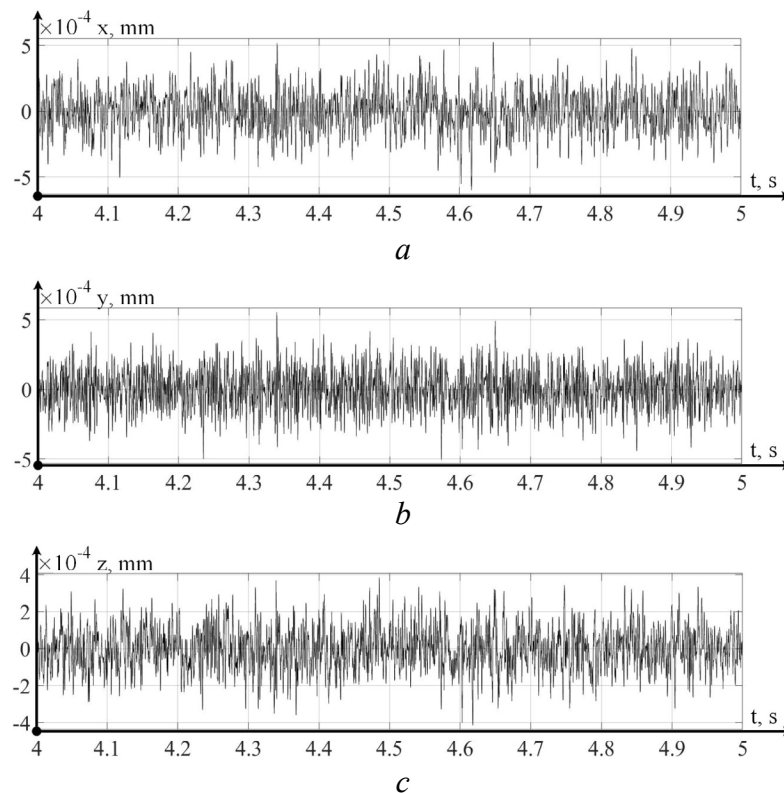the wear of the cutting wedge, at each of eight steps, the actual wear of the cutting wedge on the back face was evaluated using a inverted metallographic microscope *LaboMet-I* version 4, equipped with wide-angle lenses 5/20, having a 20 mm linear field of view, and a digital camera for microscopes *Ucam-1400* with a 1.4 μm×1.4 μm matrix. The microscope appearance and measurement results are shown in Fig. 6 and 7.

A portion of the cutting tool wear measurement results is shown in Fig. 7

As shown in Fig. 7, the back face wear measurements were 0.3 mm for the first trial and 0.33 mm for the second trial. The complete measurement results are presented in the Table 1 below.

The measurement results are shown in Fig. 8.

The wear curve development of the cutting tool, illustrated in Fig. 9, identifies three characteristic measurement points. These points will be used later for parametric identification of virtual models within the digital twin.

Now, consider the relationship between the cutting tool wear and the surface quality of the machined part. To perform this assessment, a *Contour ELITE* optical three-dimensional microscope and a *T4HD* contour profile recorder (shown in Fig. 9) were used.

Due to the physical size of the measuring equipment (*Contour ELITE* optical three-dimensional microscope and *T4HD* contour profile recorder), surface quality measurements could not be performed directly on the machine. To facilitate quality assessment, it was necessary to isolate the regions of interest. Therefore, each step of the experiment, where tool wear was measured, also included the creation of a corresponding evaluation surface. Considering that the shaft was ground during the experiment, it was convenient to measure tool wear after each tool stroke along the shaft and to design each step such that the processed surface from the previous step was preserved.

After a series of experiments in which force response and the power of irreversible transformations (temperature in the cutting zone) were also measured, the resulting machined shaft exhibited a conical shape with a discretely decreasing radius, as shown in Fig. 10.
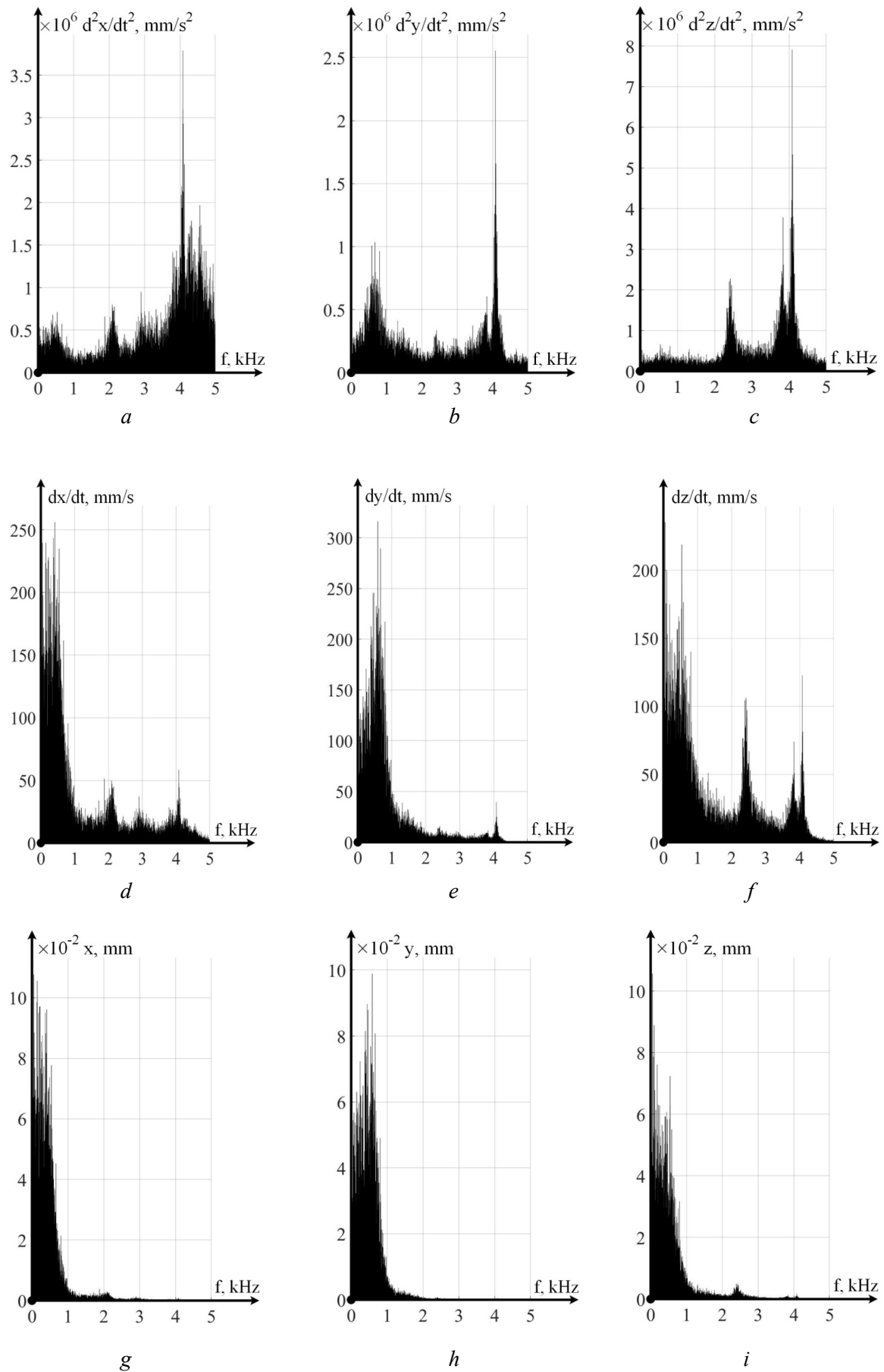
Fig. 5. Power spectra of cutting tool vibration activity signals for cutting at a speed of 150 m/min:
a, *b*, *c* – in the axial direction; *d*, *e*, *f* – in the radial direction; *g*, *h*, *i* – in the tangential direction
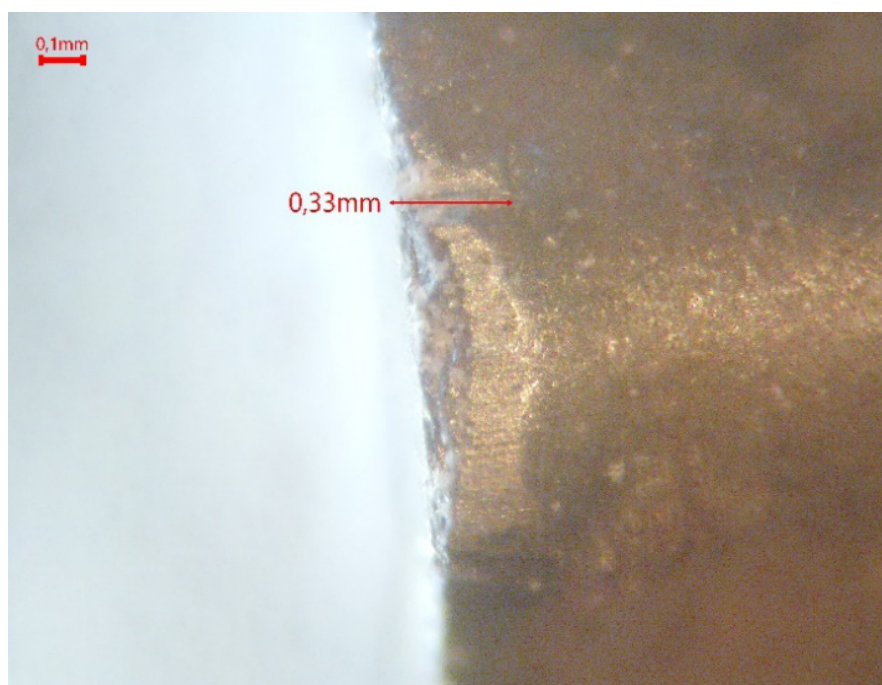
Fig. 6. The appearance
of the microscope

Fig. 7. Photograph with measured wear value

Table 1

Data on tool wear during processing

Cutter travelled distance, m	0	202	552	840	1,375	2,010	3,061
Wear of the cutting plate, mm	0.01	0.11	0.20	0.23	0.24	0.26	0.36

Following machining on the lathe, this shaft was sectioned into smaller pieces, each representing the surface quality achieved at a specific level of tool wear (Fig. 11).

These shaft sections were then used to evaluate the quality of the surface machined by tools with different degrees of wear using both the *T4HD* contour profile recorder and the *Contour ELITE* optical three-dimensional microscope.

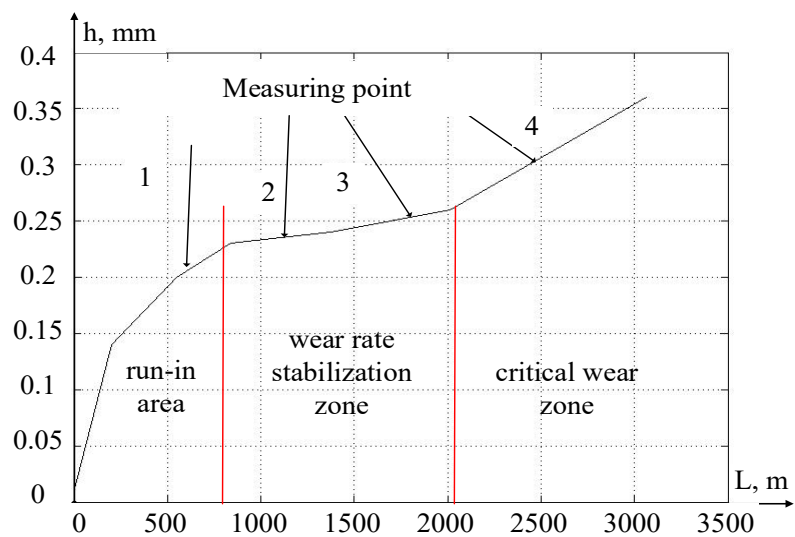*Fig. 8*. Measured wear curve of the cutting tool

a   *b*

Fig. 9. Measuring device:
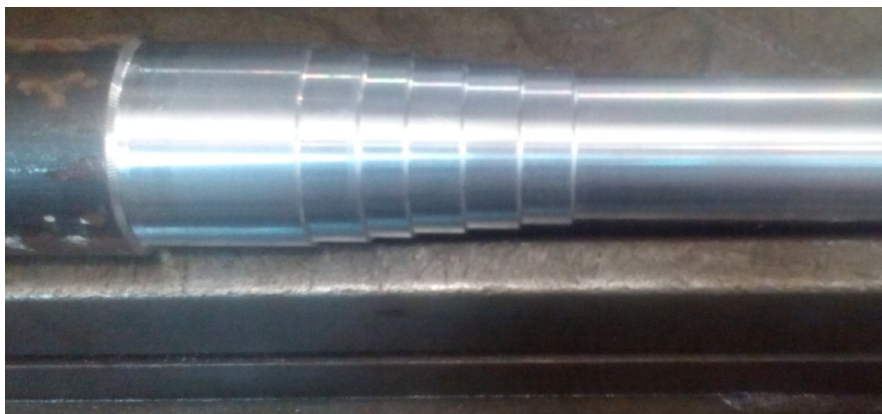*a* – contour profile recorder *T4HD*; *b* – microscope *Contour ELITE*

Fig. 10. Part after the experiment is complete

Fig. 11. The part prepared for measurements

Based on the data acquired from the *Contour ELITE* optical microscope, the changes in the R_a and R_z parameters (units of measurement: μm) across the experimental steps are shown in Table 2.

Table 2

Results of measuring *Contour ELITE* roughness indicators

Parameters	Point 1	Point 2	Point 3	Point 4
R_z on the y axis (μm)	26.186	21.347	22.898	18.152
R_a on the y axis (μm)	2.41	1.493	1.794	2.975

As the data in Table 2 reveals, there is no clear, consistent trend in the change of R_a and R_z. A significant increase in the arithmetic mean deviation of the profile from the mean line along the y-axis can be observed, with some fluctuations at the fifth step. However, the changes in R_a and R_z along the x-axis are not substantial, and, in general, these two indicators even decrease along this axis.

In the case shown in Fig. 12, obtained at the second measurement point, the changes in the part's profile along the feed direction (y-axis) are clearly due to the size of the tool's step movement along the feed line. Decreasing the feed rate will reduce the R_a and R_z parameters along the y-axis, while increasing the feed rate will increase them. To illustrate this more clearly, a 3D model of the machined surface obtained on the *Contour ELITE* microscope at the second experimental point is provided (Fig. 13).
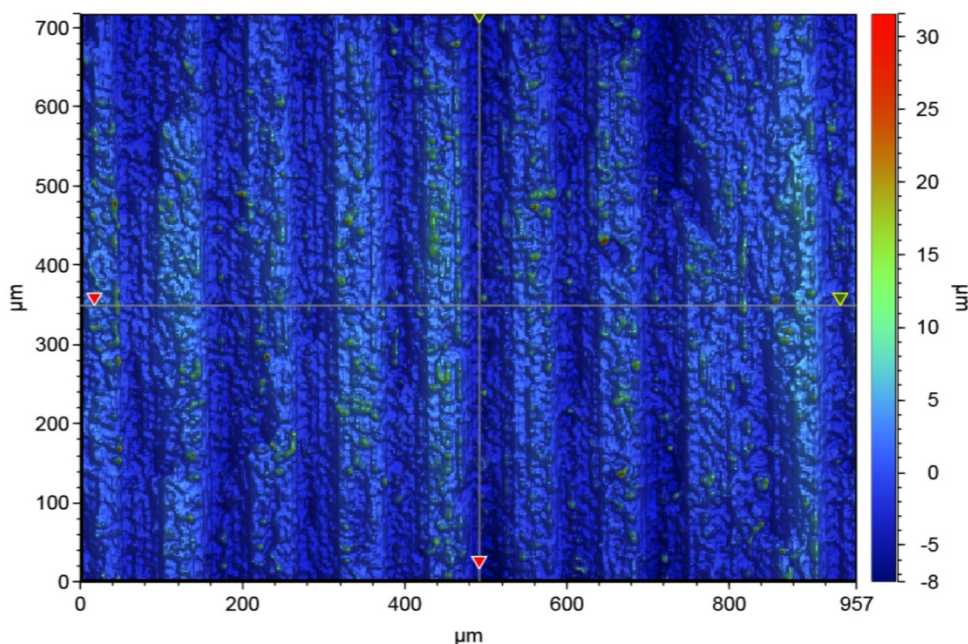

Fig. 12. Photograph of the machined surface, obtained with a microscope
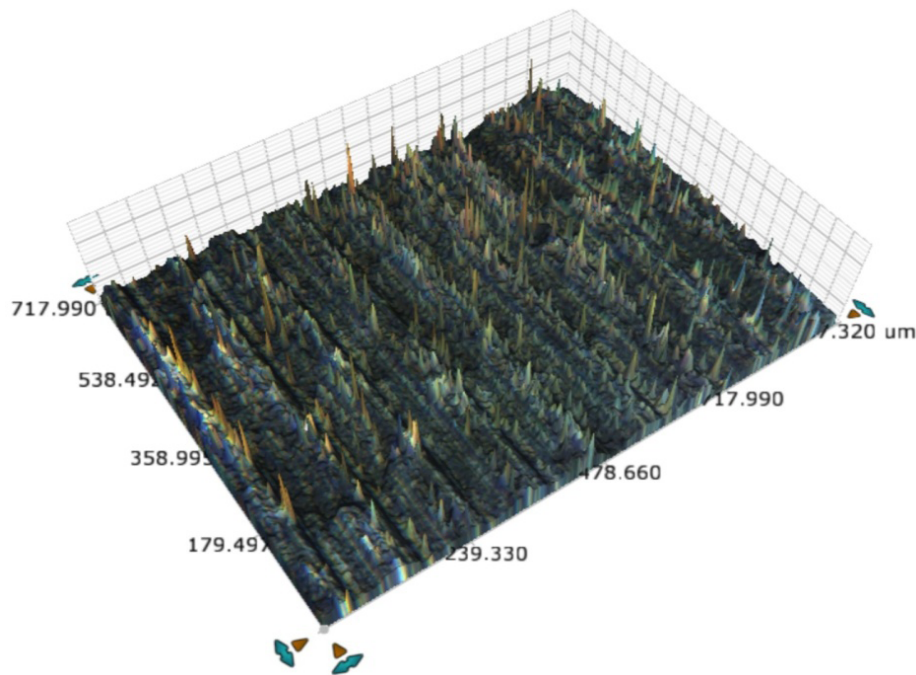*Contour ELITE*, after the first step of the experiment

Fig. 13. 3D model of the surface after the first step of the experiment

To illustrate the appearance of a surface machined with near-catastrophic tool wear, consider a photograph of the machined surface obtained using the *Contour ELITE* microscope at the fourth experimental point (Fig. 14).
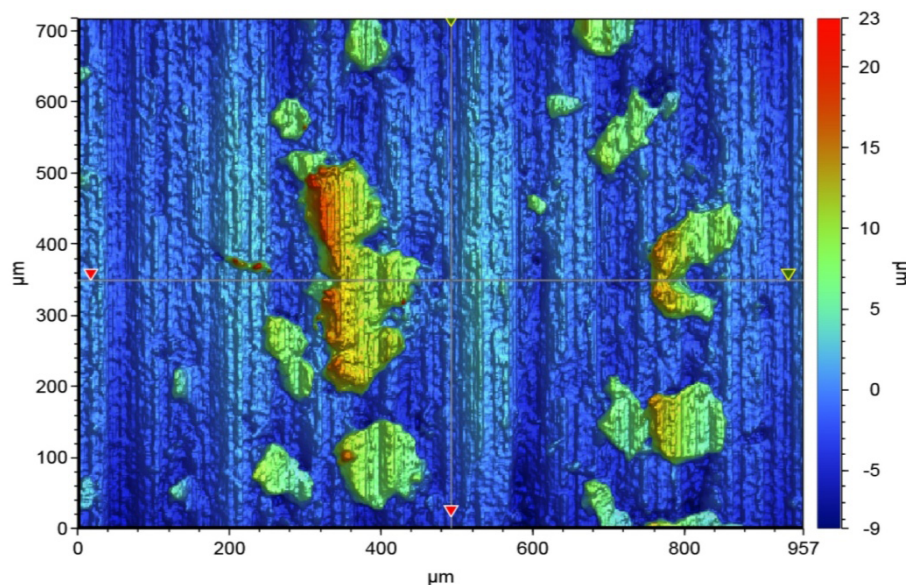
Fig. 14. Photograph of the machined surface, obtained with a microscope
Contour ELITE, after the sixth step of the experiment

As shown in Fig. 14, the quality of the machined surface significantly deteriorated at this step of the experiment. This is also evident from the R_a indicator along the *y*-axis, which reaches its maximum value in this case (see Table 2). While the arithmetic mean deviation of the profile from the midline along the *y*-axis is not the highest, this is explained by the specific location of the measurement axis, which did not align with the area exhibiting the greatest profile deviations. The latter case is further illustrated with a 3D model of the surface image (Fig. 15).

Fig. 15. 3D model of the surface after the sixth step of the experiment

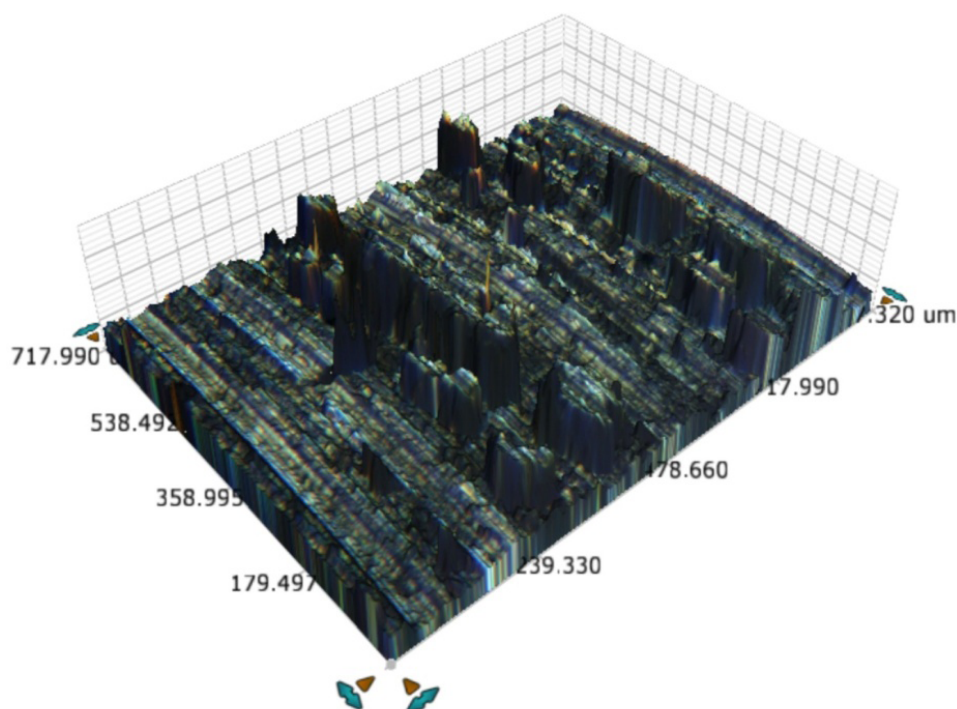Comparing the 3D model in Fig. 15 to the case in Fig. 13 indicates a significant deterioration in the quality of the machined surface. A graph summarizing the experiments is shown below (Fig. 16).
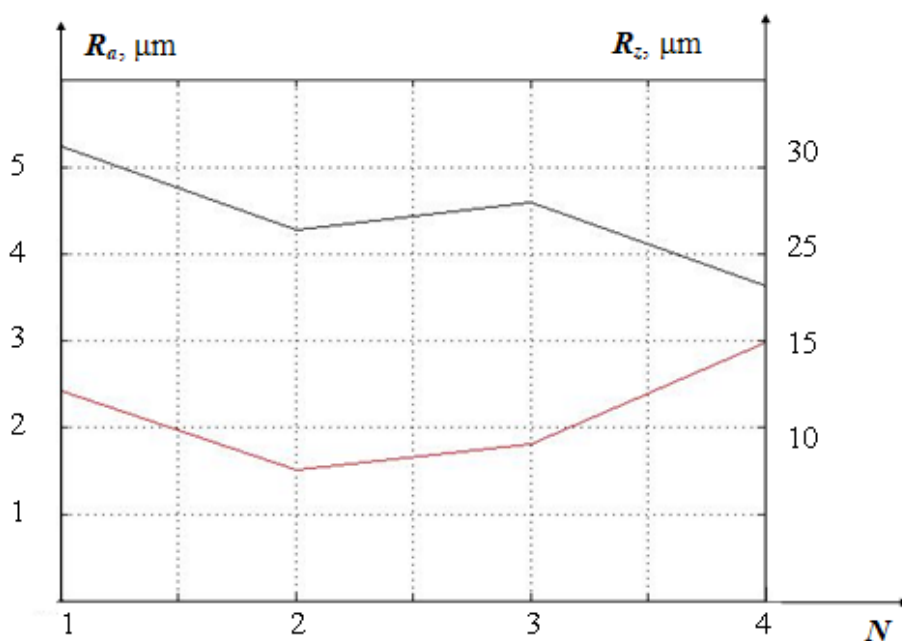
Fig. 16. Results of surface quality measurement at 4 points

As can be seen in Fig. 16, the R_a indicator is the most informative parameter. In general, the data obtained from the *Contour ELITE* optical three-dimensional microscope, particularly the 3D models, are qualitative in nature. They do not provide a clear, quantitative depiction of changes in the roughness of the machined surface. For quantitative surface quality assessment, a *T4HD* contour profile recorder was used, and its measurement protocols for a representative experimental step are shown in Fig. 17. Note that the roughness parameters were evaluated in the direction orthogonal to the feed, that is, along the *y*-axis.
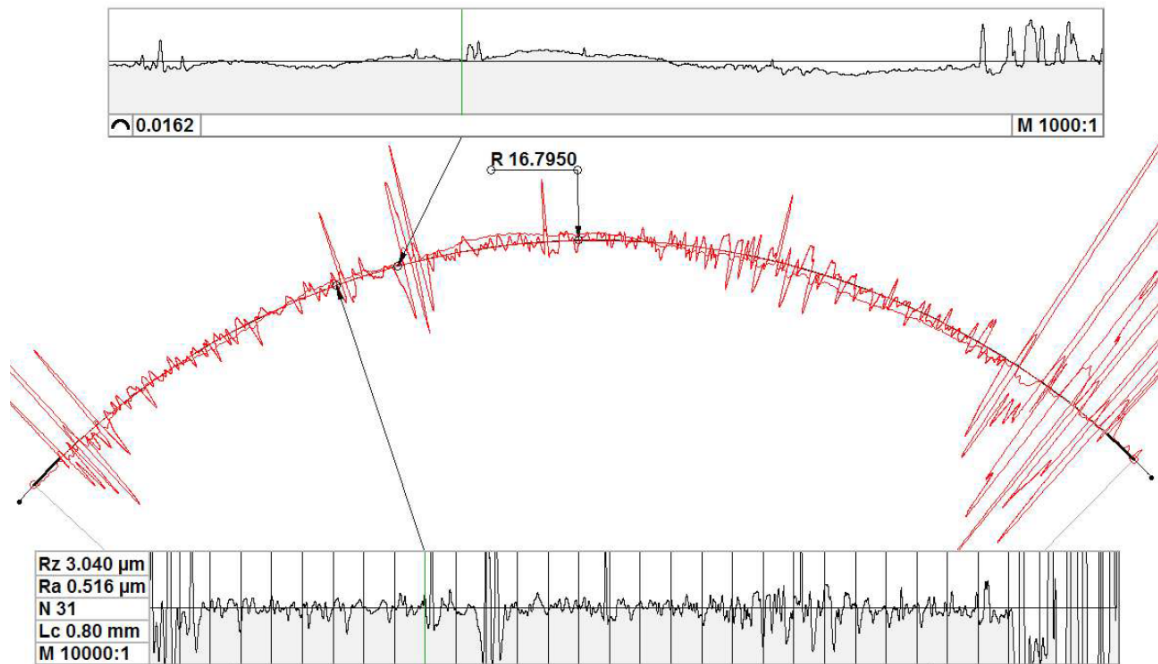
Fig. 17. Example of the protocol captured on the contour profile recorder *T4HD*

All the roughness measurement results are conveniently summarized in the following table (Table 3).

As can be seen in Table 3, both roughness parameters increase with increasing wear. A period of relative stabilization is observed after the second experimental step, followed by a sharp increase in roughness after the sixth step. The graph of the roughness change over time is shown in Fig. 18.

Table 3

Quality indicators for *T4HD* protocols

Path (m)	0	202	552	840	1375	2010	3061
R_z (μm)	4.704	3.040	3.272	3.396	3.632	5.92	9.274
R_a (μm)	0.609	0.516	0.527	0.532	0.602	0.969	1.69

Fig. 18. Change in roughness indicators along the cutting path

As shown in Fig. 18, the roughness indicators begin to increase with increasing wear. At the initial stage, the dependence between R_a, R_z on wear is decreasing, which is due to the running-in of the cutting tool. As the tool approaches the point of catastrophic wear, the increase in roughness becomes more pronounced, and the dependence becomes nonlinear.
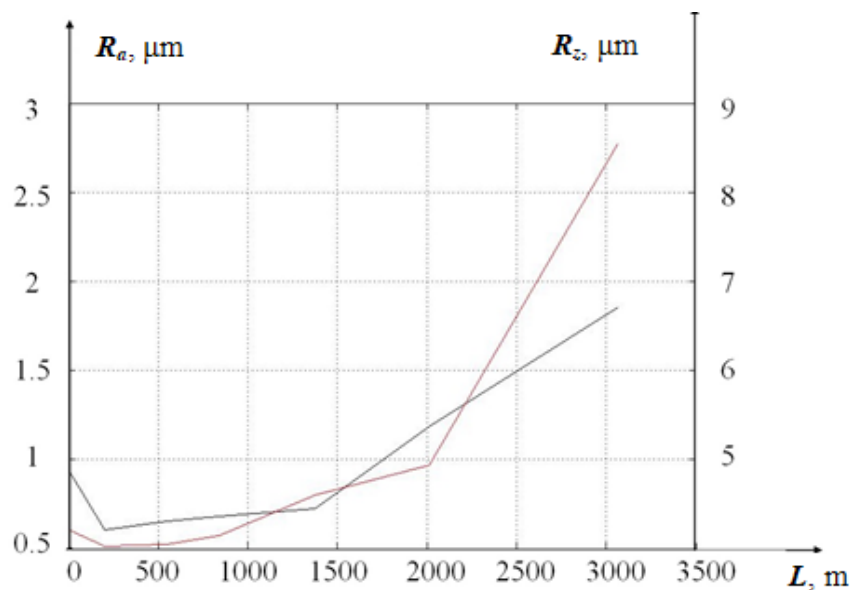
Virtual models for the digital twin

The synthesis of virtual models for the digital twin begins with constructing a cutting tool wear curve using a *Volterra* integral operator of the second kind [20]. Here, it is necessary to consider the actual path traveled by the tool, including the path deviations resulting from vibrational movements of the tool tip. This path is calculated taking into account the processed data received from the vibration monitoring system. That is, the path traveled by the tool will be determined as the sum of the calculated path, denoted as L_0, which is determined by the cutting speed and feed rate, and the virtual path traveled by the tool:

$$L_v = \sqrt{x^2 + y^2 + x^2} \ . \tag{1}$$

The simulation results of the digital twin's equation systems allow for the calculation of the predicted cutting tool wear. Modeling must account for the fact that the cause of these evolutionary transformations is related to the power and action of cutting forces, specifically the energy of irreversible transformations in the machining zone. *Volterra* integral operators of the second kind are used to model these evolutionary changes, having the following structure [21-22]:

$$h_3 = k \int_0^A w(t - \xi) N(\xi) d\xi, \tag{2}$$

where $w(t - \xi)$ is the kernel of integral operator; $N(\xi)$ is the phase trajectory of the power of irreversible transformations based on perfect work A is the work of cutting forces.

The wear depends on the intensity of irreversible transformations and its history, which is captured by the integral operator's kernel. The kernel of the integral operator is expressed as:

$$h_3 = \int_0^A \left(\beta_1 e^{\alpha_1(\xi - A)} + \beta_2 e^{\alpha_2(A - \xi)} \right) N(\xi) d\xi, \tag{3}$$

where $\left(\beta_1 e^{\alpha_1(\xi - A)} + \beta_2 e^{\alpha_2(A - \xi)} \right)$ is the sum of the kernels of an integral operator, where $\beta_1 e^{\alpha_1(\xi - A)}$ is the kernel that determines the running-in processes of the tool; $\beta_2 e^{\alpha_2(A - \xi)}$ is the kernel that determines the processes of wear; β_1, β_2, α_1, α_2 are the parameters to be identified; N is the power of irreversible transformations; A is the performance.

The power of irreversible transformations is defined as $N = R\sqrt{Vf^2 + V^2}$, where R is the cutting force.

We define the working process in the form of the following integral: $A = \int_0^t N(t)\, dt$.

In case $N = N_0 = $ const, (2) the following equation is used:

$$h_3 = N_0 \int_0^A \left(e^{\alpha_1(\xi - A)} + e^{\alpha_2(A - \xi)} \right) d\xi . \tag{4}$$

The solution for (4) will be as follows:

$$h_3 = N_0 \frac{1}{\alpha_1} \left(1 - e^{-\alpha_1 A} \right) + N_0 \frac{1}{\alpha_2} \left(e^{\alpha_2 A} - 1 \right). \tag{5}$$

If $N(t)$ is not equal to $N_0 = $ const, and taking into consideration that N_0, N_1, …, N_{n-1} due to the small size $\Delta A = A_k - A_{k-1}$ are values close to constants, we obtain the following approximate sum describing the integral operator (5):

$$h_3 = \frac{\beta_1}{\alpha_1}\left[-N_0 e^{-\alpha_1 A} - (N_1 - N_0)e^{\alpha_1(A_1 - A)} - (N_2 - N_1)e^{\alpha_1(A_2 - A)} - \ldots\right.$$

$$\left. - (N_{n-1} - N_{n-2})e^{\alpha_1(A_{n-1} - A)} + N_{n-1}\right] +$$

$$+ \frac{\beta_2}{\alpha_2}\left[-N_0 e^{\alpha_2 A} + (N_1 - N_0)e^{-\alpha_2(A - A_1)} + (N_2 - N_1)e^{-\alpha_2(A - A_2)} + \ldots\right.$$

$$\left. + (N_{n-1} - N_{n-2})e^{-\alpha_2(A - A_{n-1})} - N_{n-1}\right], \tag{6}$$

where β_1, β_2, α_1, α_2 are the parameters identified in the wear calculation model, based on the results of preliminary experiments.

The graph of the cutting tool wear development along the back edge based on the calculated data is shown in Fig. 19.
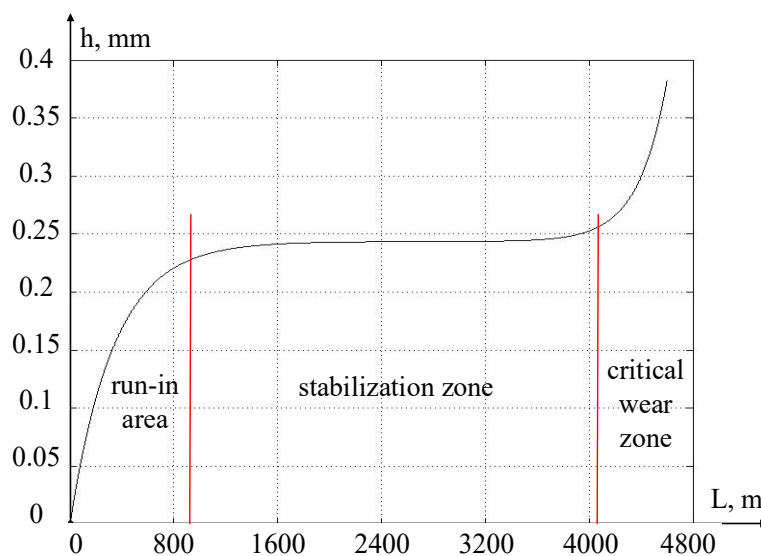

Fig. 19. Calculated cutting tool wear curve

A comparative analysis of Fig. 8 and 19 shows that the critical wear zone begins earlier in Fig. 8 than in Fig. 19. This discrepancy is attributed to the chip formation process. During machining, we deliberately allowed cutting to occur with strong vibrations resulting from the accumulation of flow chips. Consequently, these vibrations caused changes in the contact between the tool back face and the workpiece, leading to the appearance of new elemens in the wear zone.

As can be seen in Figs. 8 and 19, the wear development curve of the cutting tool along the workpiece is divided into three distinct areas:
  – the run-in area, where initial tool wear is established;
  – the area of wear stabilization, where the rate of wear increases slowly;
  – the area of formation of critical wear, where the rate of tool wear increases rapidly.

As the fundamental virtual model for a digital twin, we will adopt a system of nonlinear equations. The of the cutting force on the temperature-speed coefficient of cutting will be represented as a decreasing exponential dependence:

$$\rho = \rho_0 \left(1 + \mu e^{-\alpha_\mu \left(V_c - \frac{dz}{dt}\right)}\right), \tag{7}$$

where ρ_0 is the lowest value ρ (the coefficient that depends on temperature and characterizes the chip pressure on the front edge of the cutting wedge); μ is a coefficient showing the curvature of the exponential decrease ρ as the contact temperature increases; α_μ is a steepness coefficient of the characteristic ρ; $\left(V_c - \frac{dz}{dt}\right)$ is a real cutting speed.

Taking into account Equation (7), the cutting force can be expressed as the following:

$$F = \rho_0 \left(1 + \mu e^{-\alpha_1 \left(V_c - \frac{dz}{dt}\right)}\right)(a_p - y) \int_{t-T_v}^{t} \left(V_f - \frac{dx}{dt}\right) dt, \tag{8}$$

where $(a_p - y)$ is a real cutting depth; $\int_{t-T_v}^{t} \left(V_f - \frac{dx}{dt}\right) dt$ is a real feed.

The outward force originating from the cutting zone, which depends on wear of the tool along the back surface and the thermal expansion of the workpiece material, is expressed as:

$$F_h = \left(\sigma_0 + k_Q^F Q_h\right) h_3 (a_p - y) e^{-K_h x}, \tag{9}$$

where σ_0 represents the ultimate strength of the processed metal in compression, kg/mm^2, depending on the temperature of the contact between the back surface of the tool Q_h and the workpiece, °C; K_h, is a coefficient that characterizes a nonlinear increase in outward force when the back surface of the tool and the workpiece come closer.

Through the main cutting edge angle φ, the resultant force can be resolved along the x and y axes of deformation as follows:

$$\begin{cases} F_h^{(x)} = \cos \varphi F_h; \\ F_h^{(y)} = \sin \varphi F_h. \end{cases} \tag{10}$$

The force component on the tool back face in the z-coordinate direction, representing the friction force, is:

$$F_h^{(z)} = k_t F_h, \tag{11}$$

where k_i is the coefficient of friction is interpreted as:

$$k_t = k_{0t} + \Delta k_t \left[e^{-K_{f1} Q_h} + e^{K_{f2} Q_h}\right]/2, \tag{12}$$

where k_{0t} is minimum value of the coefficient of friction; Δk_t is the incremental change in the friction coefficient with a change in temperature in the contact area; K_{f1} and K_{f2} are coefficients that determine the rate of decrease and increase, respectively, of the friction coefficient characteristic.

The general expression describing the force reaction resolved along the axes of deformation takes the following form:

$$\begin{cases} F_f = \chi_1 F + F_h^{(x)}; \\ F_p = \chi_2 F + F_h^{(y)}; \\ F_c = \chi_3 F + F_h^{(z)}, \end{cases} \tag{13}$$

where χ_i is the coefficient of the cutting force decomposition on the *i*-axis of tool deformation.

The deformation movement model of the tool tip is as follows:

$$\begin{cases} m\dfrac{d^2x}{dt^2} + h_{11}\dfrac{dx}{dt} + h_{12}\dfrac{dy}{dt} + h_{13}\dfrac{dz}{dt} + c_{11}x + c_{12}y + c_{13}z = F_f; \\[3mm] m\dfrac{d^2y}{dt^2} + h_{21}\dfrac{dx}{dt} + h_{22}\dfrac{dy}{dt} + h_{23}\dfrac{dz}{dt} + c_{21}x + c_{22}y + c_{23}z = F_p; \\[3mm] m\dfrac{d^2z}{dt^2} + h_{31}\dfrac{dx}{dt} + h_{32}\dfrac{dy}{dt} + h_{33}\dfrac{dz}{dt} + c_{31}x + c_{32}y + c_{33}z = F_c, \end{cases} \qquad (14)$$

where m [kg·s^2/mm]; h [kg·s/mm]; c [kg/mm] are the inertia, dissipation, and stiffness matrices, respectively.

The differential equation describing the temperature transfer through back surface of the tool from the previous spindle revolution to the current contact zone between the tool and the workpiece is given by:

$$T_1 T_2 \frac{d^2 Q_h}{dt^2} + (T_1 + T_2)\frac{dQ_h}{dt} + Q_h = kN, \qquad (15)$$

where $T_1 = \dfrac{\lambda}{\alpha_1 V_c}$, $T_2 = \dfrac{h_3}{\alpha_2}$ are time constants; $k = \dfrac{k_Q \lambda h_3}{\alpha_1 \alpha_2 V_c}$ is the transmission ratio; α_1, α_2 are identifiable dimensionless scaling parameters of the integral operator; λ is the thermal conductivity coefficient; k_Q is the coefficient characterizing the conversion of irreversible transformation power into temperature; $N = F_c(t - T_v)\left(V_c - \dfrac{dz(t - T_v)}{dt}\right) = \left(\chi_3 F(t - T_v) + F_h^{(z)}(t - T_v)\right)\left(V_c - \dfrac{dz(t - T_v)}{dt}\right)$ is the force of irreversible transformations.

Thus, the system of equations (3) through (15) constitutes a virtual mathematical model for the digital twin of the metalworking process on a metal-cutting machine.

Research Results and Discussion

The most promising approach for parametric identification of virtual digital twin models is the use of data acquired from a vibration monitoring system [20]. Here, from the complete dataset, we propose focusing on so-called scattering ellipses, which can be obtained directly from the recorded vibration acceleration signal.

Let us consider the scattering ellipses for the cases presented in Fig. 8, identifying the parameters of the digital twin model from these data. The results of comparing these two methods for calculating scattering ellipses, for equal values of cutting wedge wear, are shown in Fig. 20.

As seen in Fig. 20, the span of the scattering ellipse axes coincides almost exactly. However, the vibration dispersion for the real machine is significantly higher. This is attributed to the presence of vibration activity not only from the cutting process but also from other system carriers within the real machine. Modeling all supporting systems in conjunction with the cutting system remains an unresolved task.

To evaluate the quality of the surface obtained during cutting, only the vibration activity coordinate of the cutting tool along the *y*-axis was analyzed. This choice is based on the fact that vibrations at the cutting tool tip along the *z*- and *x*-axes will be attenuated during longitudinal turning, which forms the basis for modeling the cutting system. However, in other metalworking operations, the vibration signal in other directions can also be analyzed. To analyze the quality of the surface obtained by cutting, we needed to process the data to remove any constant component, considering only the vibrations within a defined time range. For this purpose, we developed a program that allows us to analyze the quality of the surface obtained during cutting, both within the digital twin system and based on data acquired by the vibration monitoring system. This resulted in a sufficiently powerful computational tool that can subsequently be used for parametric identification of virtual digital twin models on real metalworking machines.
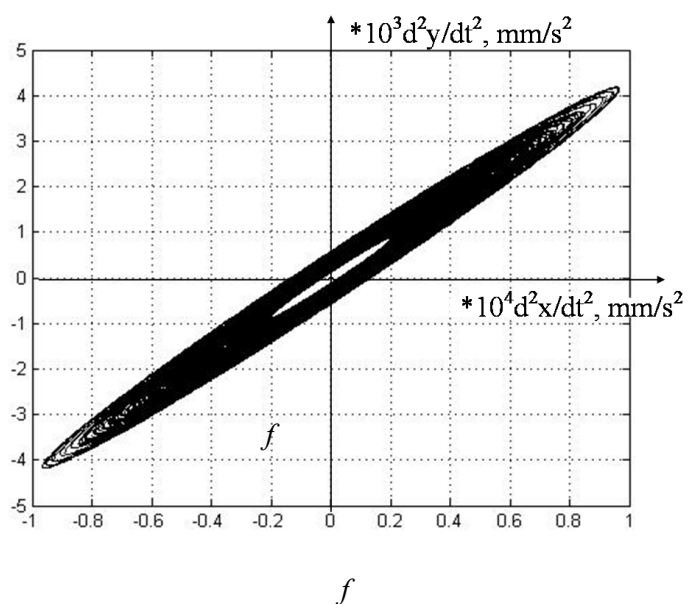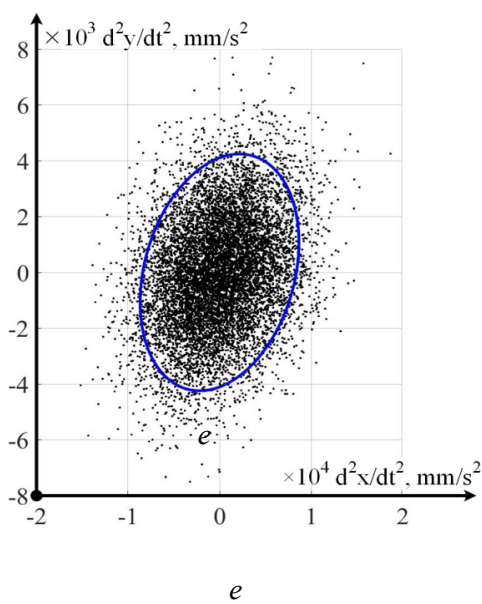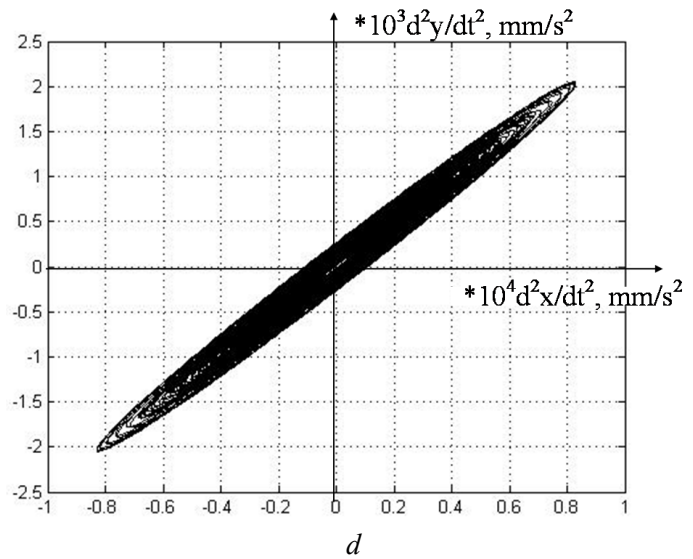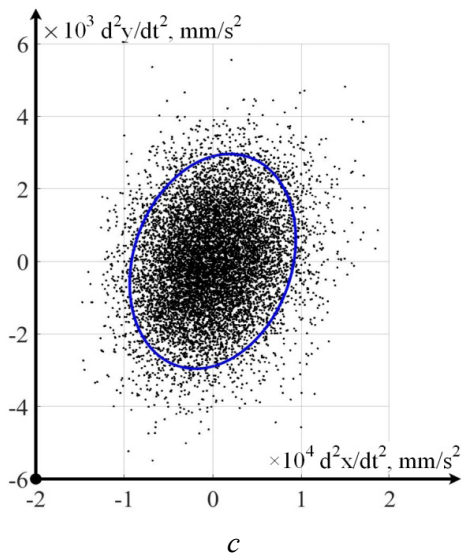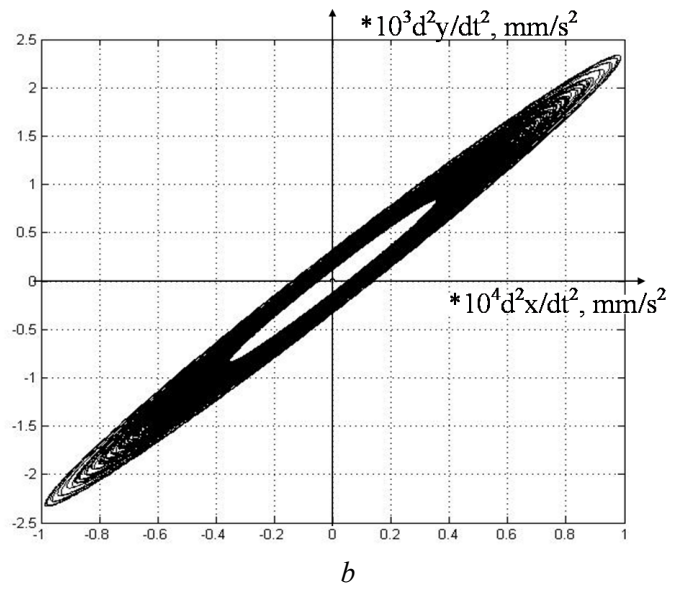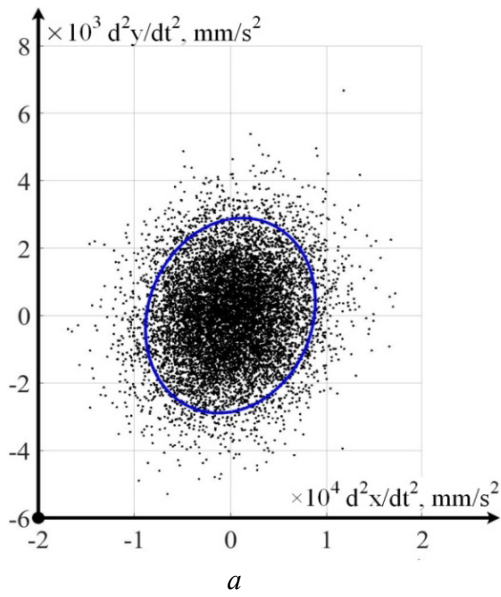
Fig. 20. Ellipses of dispersion of the "rose" of vibrations:

a, b – in the **X/Y** plane with a wear value of **h** = 0.24 mm; *c, d* – in the **X/Y** plane with a wear value of **h** = 0.27 mm; *e, f* – in the **X/Y** plane and a wear and tear **h** = 0.32 mm

The simulation results of the deformation motion along the *y*-axis, as well as the points at which the surface roughness was evaluated using the R_a indicator, are presented in the figures below (see Figs. 21-23). Fig. 21 illustrates the method for calculating machining quality based on the R_a indicator for a cutting scenario with 0.11 mm of cutting tool wear on the back face.

As seen in Fig. 21, the calculation was performed using data obtained from the model, but not from the first second, i.e., the start of the simulation, but rather from the time when the cutting process reached a steady state. In the resulting sample, we only considered the minimum and maximum values, which were used to calculate the roughness parameter, which in this case is equal to 1.26 μm.
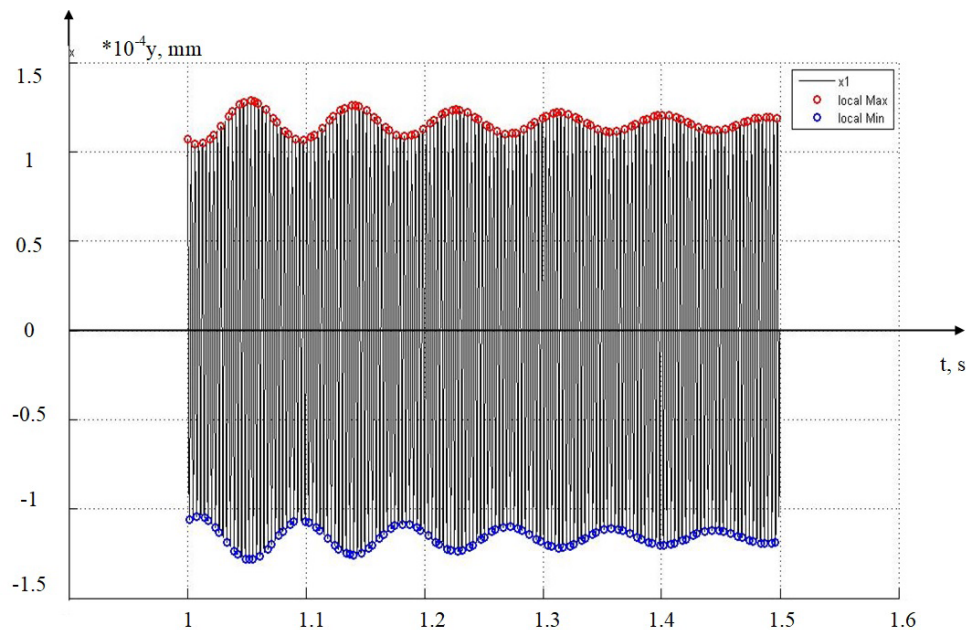
Fig. 21. Example of calculating the quality index for the case of cutting with a wear of 0.11 mm
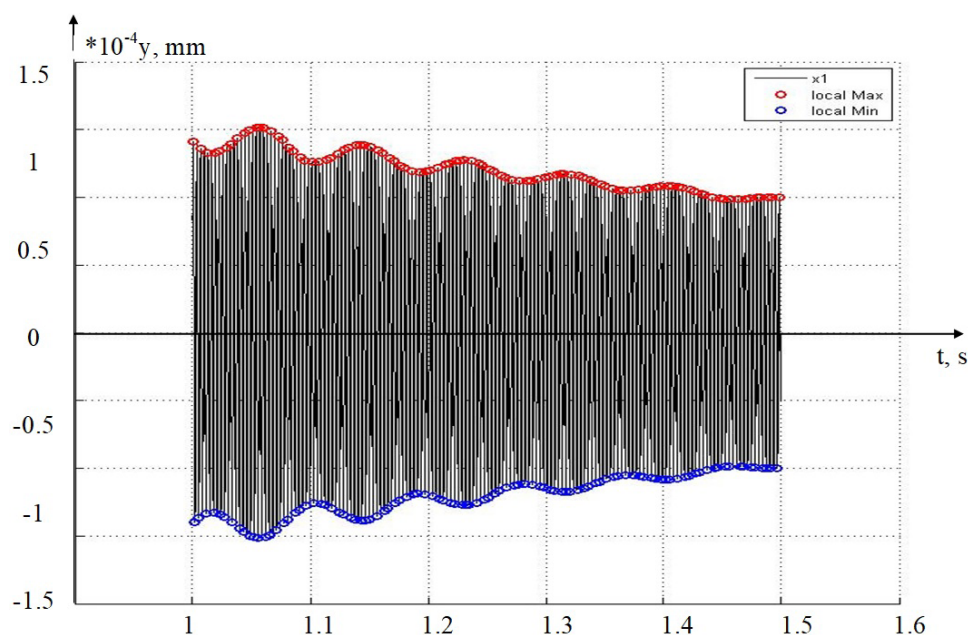
Fig. 22. Example of calculating the quality index for the case of cutting with a wear of 0.29 mm
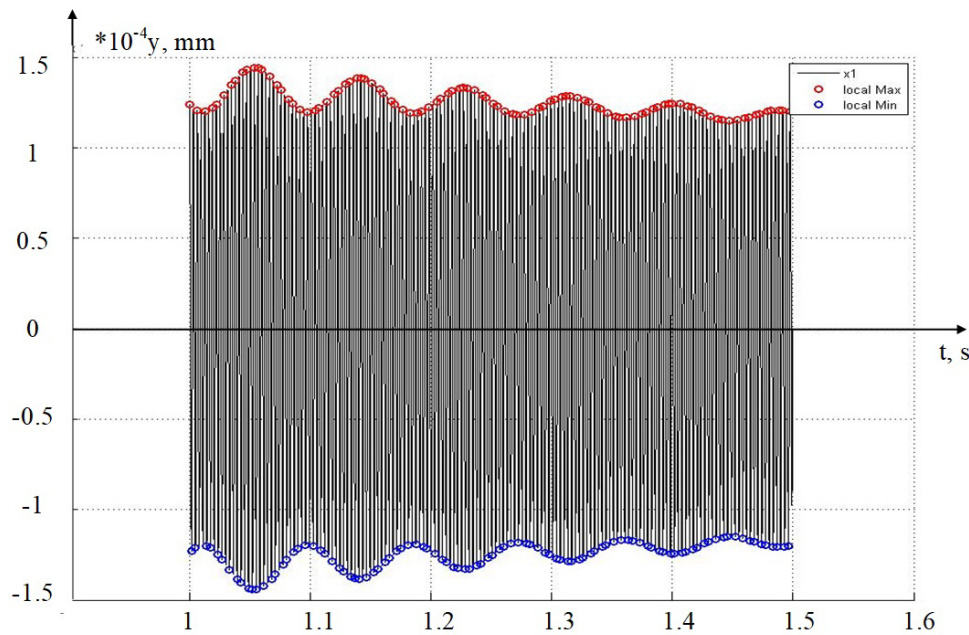
Fig. 23. Example of calculating the quality index at **h** = 0.314 mm

The simulation results for the coordinate representing the deformation motions of the cutting tool tip in the radial direction, with the wear of the cutting tool along the back face of 0.29 mm, are shown in the figure below.

As can be seen from the figure, the amplitude of the deformation motions increases significantly, and for this cutting case, the calculated R_a value reaches 2.2 μm, which is substantially higher than the previous calculated values. This jump is due to the transition of the wear curve from the stabilization region to the region of critical wear.

Let's consider another cutting scenario, characterized by the wear of the cutting tool along the back face of 0.344 mm. The simulation results for the **y**-coordinate for this case are shown in Fig. 23.

A comparison of Figs. 22 and 23 shows an even greater increase in the vibration amplitude of the cutting tool, including in the radial direction. The calculated surface quality parameter for this case reached a value of 4.17 μm, which is a very large value for the case of metal turning and can only be considered as a roughing or pre-finishing option.

In total, we conducted nine experiments to construct the curve of surface quality variation during cutting. For clarity, let's consider both the experimental evaluation and the model evaluation of surface quality variation. To do this, let's examine the variation of R_a for the case of experimental data, based on the interpretation of this parameter using the data presented in Figs. 8 and 19.

The interpretation of the data from Table 4, presented as a combined graph of two characteristics, is shown in the figure below.

As seen in Fig. 25, in this case of comparing simulation results with experimentally obtained results, both characteristics exhibit a very high degree of similarity. There is a slight discrepancy in the region of average values of the value characterizing the wear of the cutting tool along the back face, but overall, the characteristics are almost identical.

T a b l e 4

Values of the quality indicator *Ra* (experimental and modeled)

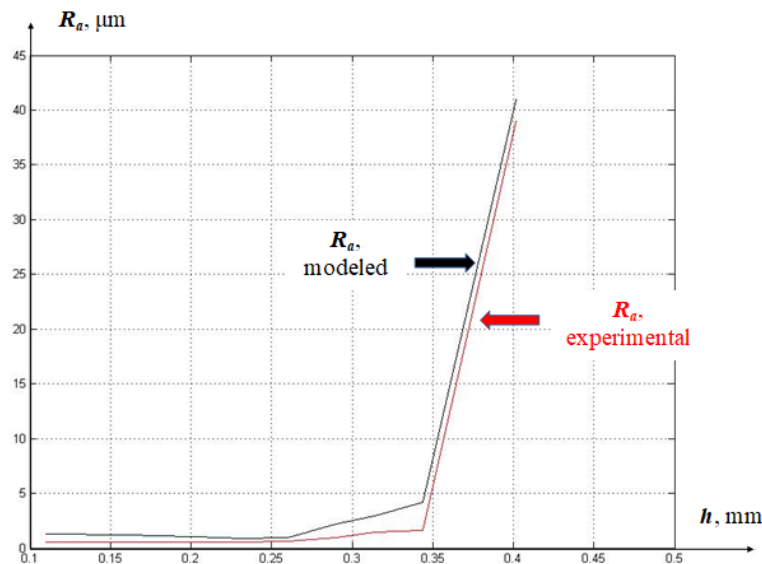| Wear (mm)	0.11	0.16	0.22	0.23	0.26	0.29	0.314	0.344	0.402
Ra (μm) (modeled)	1.26	1.22	0.96	0.84	0.98	2.2	2.9	4.17	41
Ra (μm) (experimental)	0.516	0.52	0.53	0.532	0.602	0.97	1.45	1.6	39

Fig. 24. Dependence of the surface quality obtained during
cutting on the cutting tool wear

It should be noted that both the model and experimental characteristics show stabilization and even some decrease in the R_a value in the stabilization area of the cutting tool wear curve (see Fig. 24).

The digital twin technology relies on the widespread use of virtual mathematical models, the numerical simulation of which can predict the development of various processes in technical systems. The importance of such a prediction largely depends on the accuracy of the models used in the simulation, which in turn require constant parametric adjustment of the parameters. Primarily, such adjustment is associated with the increasing wear of the cutting tool, which must also be modeled in the digital twin system. The particular cutting case that we have considered only allows us to conclude the possibility of predicting the surface quality obtained during cutting based on calculations performed on virtual models of the digital twin.

Overall, the purpose of the study set at the beginning of the paper has been achieved, mainly due to the introduction of a module for calculating the increase in cutting tool wear into the model, and also due to the parametric identification of the remaining model parameters. Studies have shown that the accuracy of predicting the dependence of the surface quality obtained during cutting on the cutting tool wear is sufficiently high for this particular case. The largest discrepancies between the modeled and experimental characteristics are observed in the range from 0.25 mm to 0.36 mm of cutting tool wear. This range is characterized by the largest deviation of the experimental and simulated curves of cutting tool wear (see Figs. 8 and 19).

In the example we provided, the cutting tool wear curve along the cutting path behaved classically, and three wear areas could be identified on it, as well as on the simulated characteristic. However, this is a specific case, and the cutting tool wear may increase abruptly, in a jump, due to various random factors. For this case, it is necessary to integrate an intelligent subsystem for recognizing such non-standard cases of cutting tool wear development into the parameter identification system of the virtual models of digital twins.

Conclusion

This work considered the issues of assessing the interrelationship between cutting tool wear and the quality of the surfaces obtained during cutting. The quality of the surfaces obtained during cutting was assessed using the R_a value, which proved to be the most informative for the case under consideration, both for processing experimental data and for simulating. Given the dependencies obtained in Fig. 24, it can be asserted that predicting the quality of the surface of parts obtained by cutting based on the results

of modeling systems of equations is a fully achievable task. The research results showed that improving the accuracy of predicting the surface quality obtained during metal cutting is directly dependent on the accuracy of modeling the cutting tool wear curve.

Some discrepancy in the results is generally acceptable, and in terms of implementing a digital twin system, as well as subsequently refining the model parameters, it is possible to use intelligent recognition algorithms that can be tuned to the difference between the predicted and actual value of cutting tool wear.

References

1. Suslov A.G. *Kachestvo poverkhnostnogo sloya detalei mashin* [The quality of the surface layer of machine parts]. Moscow, Mashinostroenie Publ., 2000, 320 p. ISBN 5-217-02976-5.

2. Gimadeev M.P., Li A.A. Analiz avtomatizirovannykh sistem opredeleniya parametrov sherokhovatosti poverkhnosti na osnove dinamicheskogo monitoringa [Analysis of automated surface roughness parameter support systems based on dynamic monitoring]. *Advanced Engineering Research*, 2022, no. 2 (22), pp. 116–129. DOI: 10.23947/2687-1653-2022-22-2-116-129.

3. Tugengol'd A.K., Luk'yanov E.A., Voloshin R.N., Bonilla V.F. Intellektual'naya sistema monitoringa i upravleniya tekhnicheskim sostoyaniem mekhatronnykh tekhnologicheskikh ob"ektov [Intelligent system for monitoring and controlling the technical condition of mechatronic process facilities]. *Vestnik Donskogo gosudarstvennogo tekhnicheskogo universiteta = Vestnik of Don State Technical University*, 2020, no. 2 (20), pp. 188–195. DOI: 10.23947/1992-5980-2020-20-2-188-195.

4. Zakovorotnyi V.L., Gvindjiliya V.E. Influence of speeds of forming movements on the properties of geometric topology of the part in longitudinal turning. *Journal of Manufacturing Processes*, 2024, no. 112, pp. 202–213. DOI: 10.1016/j.jmapro.2024.01.037.

5. Altintas Y., Kersting P., Biermann D., Budak E., Denkena B., Lazoglu I. Virtual process systems for part machining operations. *CIRP Annals*, 2014, no. 2 (63), pp. 585–605. DOI: 10.1016/j.cirp.2014.05.007.

6. Altintas Y. *Manufacturing automation: metal cutting mechanics, machine tool vibrations, and CNC design*. Cambridge, New York, Cambridge University Press, 2012. 366 p.

7. Altintaş Y., Budak E. Analytical prediction of stability lobes in milling. *CIRP Annals*, 1995, vol. 1 (44), pp. 357–362. DOI: 10.1016/S0007-8506(07)62342-7.

8. Kabaldin Y.G., Shatagin D.A. Artificial intelligence and cyberphysical machining systems in digital production. *Russian Engineering Research*, 2020, vol. 40 (4), pp. 292–296. DOI: 10.3103/S1068798X20040115.

9. Chigirinsky Yu.L., Ingemansson A.R. Tekhnologicheskie aspekty podgotovki tsifrovogo mashinostroitel'nogo proizvodstva [Engineering process aspects of digitalization of machine-building production]. *Naukoemkie tekhnologii v mashinostroenii = Science Intensive Technologies in Mechanical Engineering*, 2023, no. 9 (147), pp. 39–48. DOI: 10.30987/2223-4608-2023-39-48.

10. Zakovorotny V.L., Gvindjiliya V.E. Process control synergetics for metal-cutting machines. *Journal of Vibroengineering*, 2022, vol. 24 (1), pp. 177–189. DOI: 10.21595/jve.2021.22087.

11. Gong S., Li S., Zhang Y., Zhou L., Xia M. Digital twin-assisted intelligent fault diagnosis for bearings. *Measurement Science and Technology*, 2024, vol. 35 (10), p. 106128. DOI: 10.1088/1361-6501/ad5f4c.

12. Zhang Y., Ji J.C., Ren Z., Ni Q., Gu F., Feng K., Yu K., Ge J., Lei Z., Liu Z. Digital twin-driven partial domain adaptation network for intelligent fault diagnosis of rolling bearing. *Reliability Engineering & System Safety*, 2023, vol. 234, p. 109186. DOI: 10.1016/j.ress.2023.109186.

13. Li T., Shi H., Bai X., Zhang K. A digital twin model of life-cycle rolling bearing with multiscale fault evolution combined with different scale local fault extension mechanism. *IEEE Transactions on Instrumentation and Measurement*, 2023, vol. 72, pp. 1–11. DOI: 10.1109/TIM.2023.3243663.

14. Li Z., Ding X., Song Z., Wang L., Qin B., Huang W. Digital twin-assisted dual transfer: a novel information-model adaptation method for rolling bearing fault diagnosis. *Information Fusion*, 2024, vol. 106, p. 102271. DOI: 10.1016/j.inffus.2024.102271.

15. Zakovorotny V.L., Gvindjiliya V.E. Sinergeticheskii podkhod k povysheniyu effektivnosti upravleniya processami obrabotki na metallorezhushchikh stankakh [Synergetic approach to improve the efficiency of machining process control on metal- cutting machines]. *Obrabotka metallov (tekhnologiya, oborudovanie, instrumenty) = Metal Working and Material Science*, 2021, vol. 23, no. 3, pp. 84–99. DOI: 10.17212/1994-6309-2021-23.3-84-99.

16. Ryzhkin A.A. *Sinergetika iznashivaniya instrumental'nykh rezhushchikh materialov (triboelektricheskii aspekt)* [Synergetics of wear of tool cutting materials (triboelectric aspect)]. Rostov-on-Don, DSTU Publ., 2004. 323 p. ISBN 5-7890-0307-9.

17. Lapshin V.P. Turning tool wear estimation based on the calculated parameter values of the thermodynamic subsystem of the cutting system. *Materials*, 2021, vol. 21 (14), p. 6492. DOI: 10.3390/ma14216492.

18. Lapshin V., Turkin I., Dudinov I. Research on influence of tool deformation in the direction of cutting and feeding on the stabilization of vibration activity during metal processing using metal-cutting machines. *Sensors*, 2023, vol. 17 (23), p. 7482. DOI: 10.3390/s23177482.

19. Huang J., Chen G., Wei H., Chen Zh., Lv Y. Sensor-based intelligent tool online monitoring technology: applications and progress. *Measurement Science and Technology*, 2024, vol. 35 (11), p. 112001. DOI: 10.1088/1361-6501/ad66f1.

20. *Lapshin V.P., Moiseev D.V.* Opredelenie optimal'nogo rezhima obrabotki metallov pri analize dinamiki sistem upravleniya rezaniem [Determination of the optimal metal processing mode when analyzing the dynamics of cutting control systems]. *Obrabotka metallov (tekhnologiya, oborudovanie, instrumenty) = Metal Working and Material Science*, 2023, vol. 25, no. 1, pp. 16–43. DOI: 10.17212/1994-6309-2023-25.1-16-43.

Conflicts of Interest

The authors declare no conflict of interest.